

Supporting Information for

**Biodegradable iron-coordinated hollow polydopamine
nanospheres for dihydroartemisinin delivery and selectively
enhanced therapy in tumor cells**

Liang Dong,^{ab} Chao Wang,^{bc} Wenyao Zhen,^{bc} Xiaodan Jia,^b Shangjie An,^{bc} Zhiai Xu,^a Wen Zhang,^{*a} and Xiue Jiang^{*bc}

^a School of Chemistry and Molecular Engineering, East China Normal University, Shanghai 200241, China.

^b State Key Laboratory of Electroanalytical Chemistry, Changchun Institute of Applied Chemistry, Chinese Academy of Sciences, Changchun, Jilin, 130022, China

^c University of Science and Technology of China, Hefei, Anhui, 230026, China

* Corresponding authors. Email: wzhang@chem.ecnu.edu.cn, jiangxiue@ciac.ac.cn

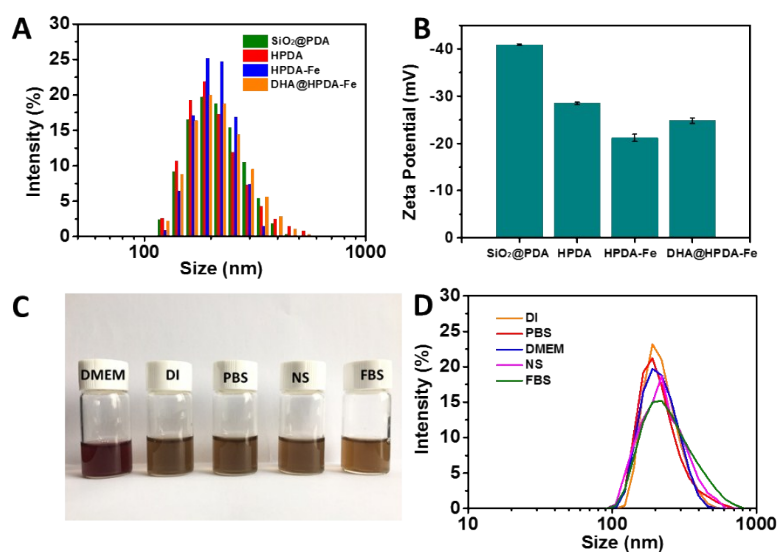


Figure S1. Hydrodynamic sizes (A) and Zeta potentials (B) of SiO₂@PDA, HPDA, HPDA-Fe, and DHA@HPDA-Fe in D.I. water, respectively. (C) Photographs of as prepared DHA@HPDA-Fe in DMEM, D.I. water, PBS, NS (saline), and FBS (80%). (D) Hydrodynamic size of DHA@HPDA-Fe in D.I. water, PBS, DMEM, NS, and FBS for five days.

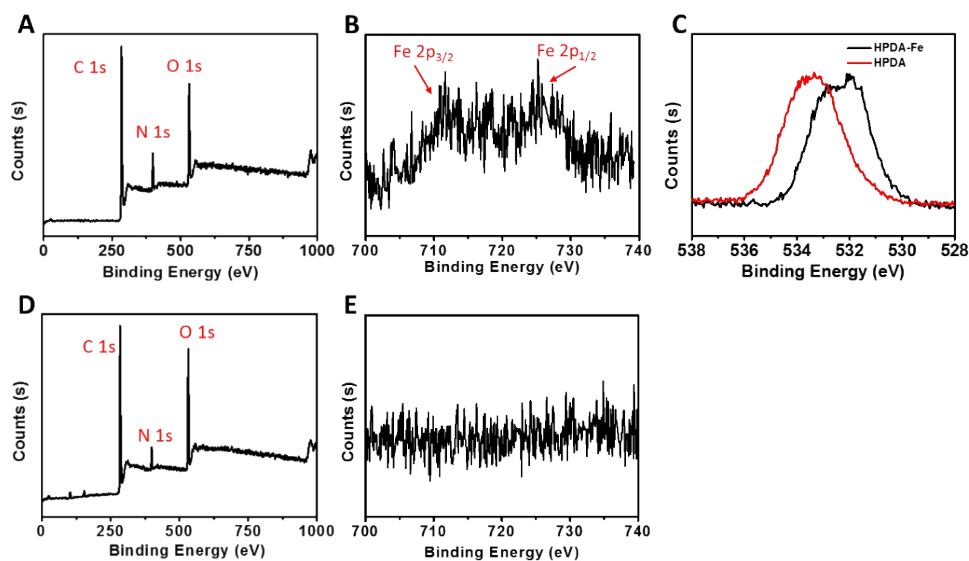


Figure S2. XPS spectrum of HPDA-Fe (A) and HPDA (D) nanospheres. Fe 2p spectrum for HPDA-Fe (B) and HPDA (E) nanospheres. (C) O1s XPS spectra of HPDA and HPDA-Fe.

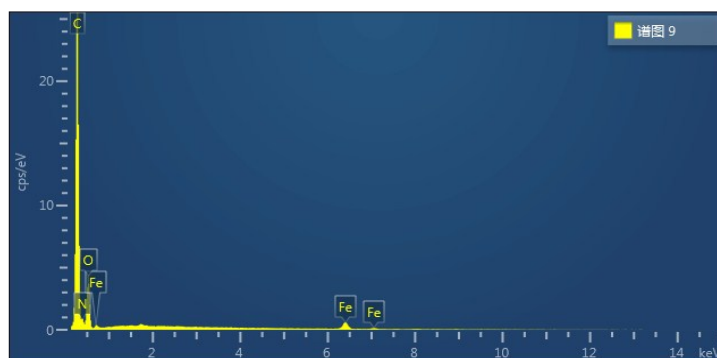


Figure S3. Energy dispersive X-ray spectrum of HPDA-Fe nanospheres.

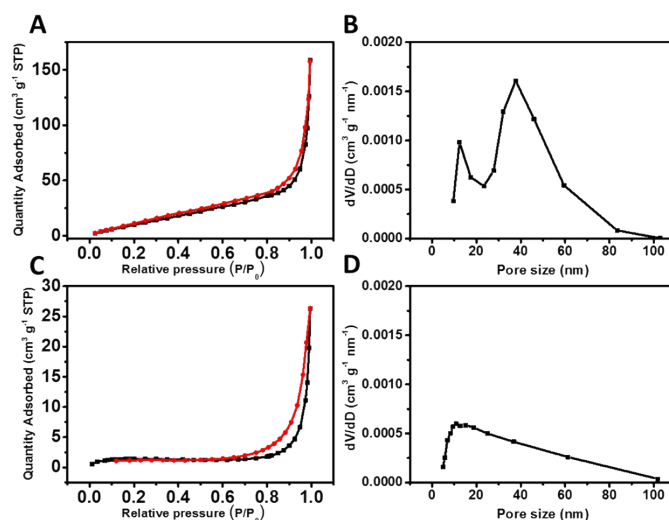


Figure S4. N₂ adsorption-desorption isotherms of HPDA-Fe (A) and DHA@HPDA-Fe (C) collected at 77 K and the corresponding pore size distribution of HPDA-Fe (B) and DHA@HPDA-Fe (D).

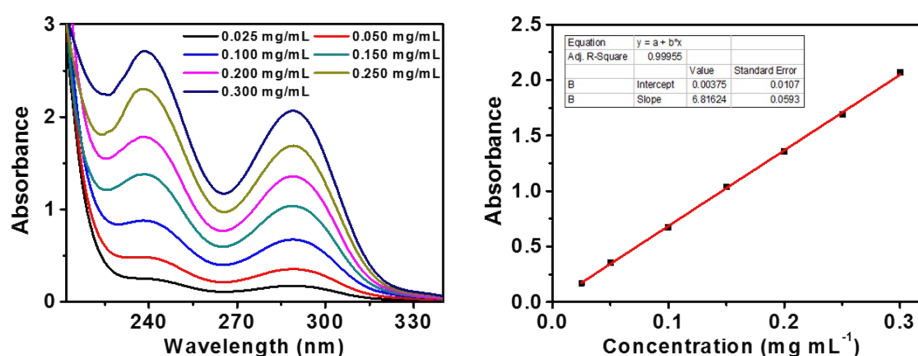


Figure S5. Quantitative measurement of DHA loading efficiency through UV-Vis method. The absorbance intensity at 290 nm was correlated with the DHA in concentration. The obtained standard curve is $y = 6.8162x + 0.0037$, $R^2 = 99.955$ (y: absorbance value at 290 nm; x: concentration of DHA).

Accordingly, DHA (4 mg mL^{-1}) was diluted to different concentrations ($0.125, 0.25, 0.5, 0.75, 1.0, 1.25, 1.5 \text{ mg mL}^{-1}$) by ethanol solution. Then, 1.0 mL DHA solution of each concentrations was

added to 4.0 mL 0.2% NaOH aqueous solution to hydrolyze at 55 °C for 30 min, then cooled down to form a stable structure of DHA derivative (UV absorbance peak was at 290 nm). The absorbance spectra of different concentrations of DHA samples were obtained by using a UV-Vis spectrometer.

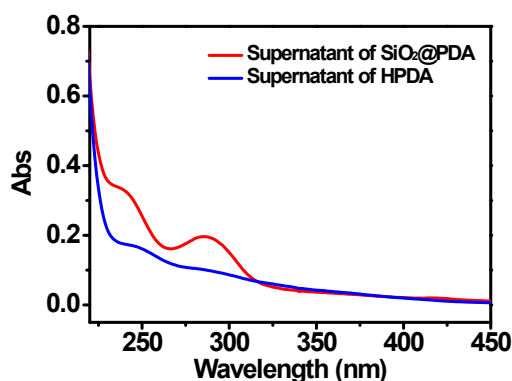


Figure S6. UV-Vis absorption spectrum of DHA after loading to SiO₂@PDA and HPDA.

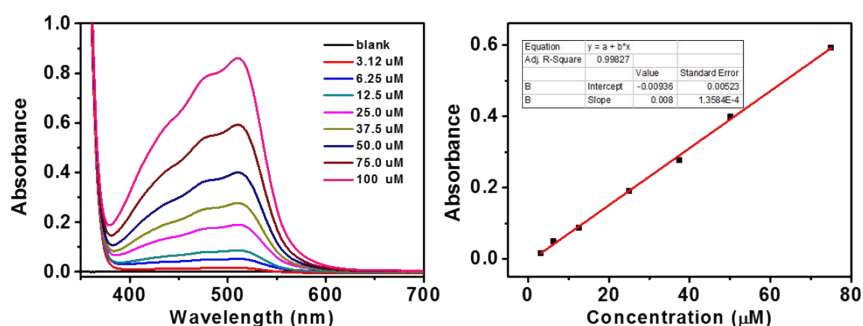


Figure S7. UV-Vis absorbance spectra with different concentrations of Fe (III) by using o-phenanthroline. The obtain standard linear equation is $y = 0.008x - 0.00936$, $R^2 = 99.827$ (y: absorbance value at 512 nm; x: concentration of Fe³⁺).

FeCl₃•6H₂O (4 mM) was diluted to different concentrations, 1 mL of each diluted sample was reduced to ferrous ion by ascorbic acid (20 mM, 1 mL) for 5 min, then 1 mL of the mixture were reacted with o-phenanthroline solution (0.1%, 1 mL) for 30 min and the red complex was produced, which absorbance peak was at 512 nm by UV-Vis absorption technique. The absorbance intensity at 512 nm was linearly correlated with the Fe ions in concentration from 3.12 µM to 100 µM.

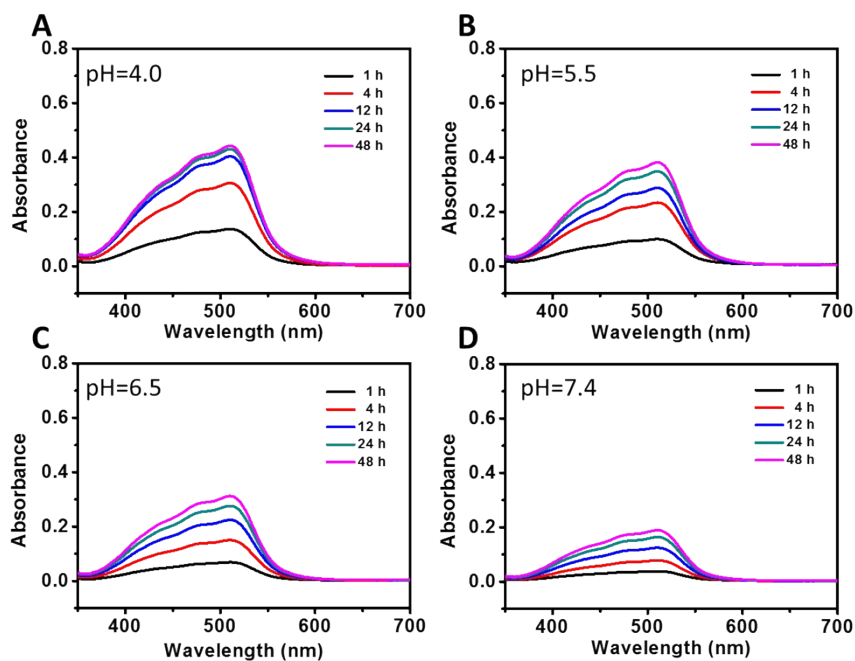


Figure S8. The absorbance spectrum of the red complex after certain time points treated with different pH (4.0, 5.5, 6.5, and 7.4) of PBS, which absorbance was at 512 nm.

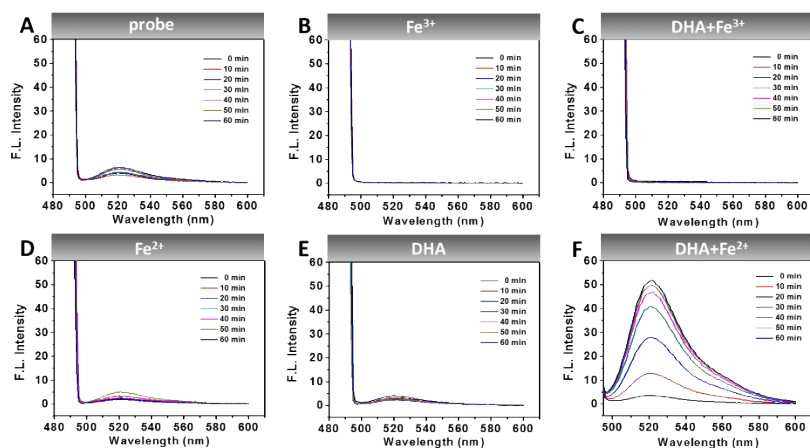


Figure S9. A-F. Detection of ROS generation in vitro, the fluorescence spectra in each group showed the intensity at different time point (0, 10, 20, 30, 40, 50, and 60 min) with 10 mM PBS buffer (pH 5.5).

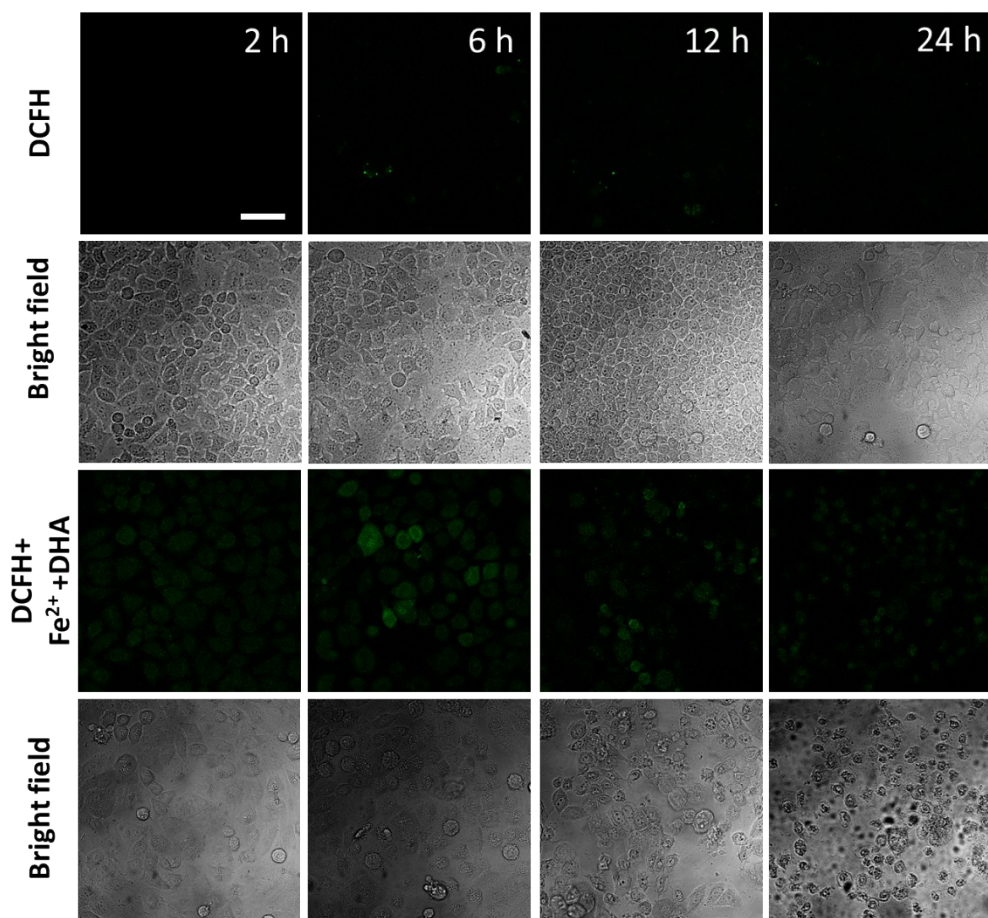


Figure S10. The CLSM images of DCFH at different time point in 24 h incubating with Fe^{2+} ($24 \mu\text{M}$) and DHA ($120 \mu\text{M}$) which concentrations are equivalent with $100 \mu\text{g mL}^{-1}$ DHA@HPDA-Fe, DCFH group served as control. (Scale bar: $75 \mu\text{m}$).

Hela cells were pretreated with DCFH-DA for 30 min, then incubated with Fe^{2+} + DHA for different time (2, 6, 12, and 24 h). From the images, it can be seen that the highest fluorescence intensity appeared after incubating with Fe^{2+} + DHA for 6 h. From the bright field images of DHA@HPDA-Fe, with the incubation time increasingly up to 24 h, the Hela cells became shrunk and gradually apoptosis.

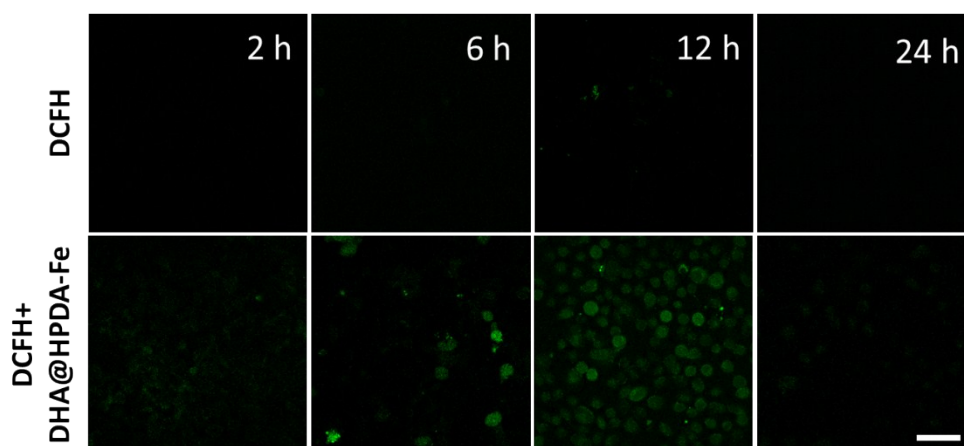


Figure S11. The CLSM images of DCFH incubating with $100 \mu\text{g mL}^{-1}$ DHA@HPDA-Fe at different time point (2, 6, 12, and 24 h), DCFH group served as control. (Scale bar: $75 \mu\text{m}$).

Hela cells were pretreated with DCFH-DA for 30 min then incubated with DHA@HPDA-Fe for different time (2, 6, 12, and 24 h). It was shown that the highest fluorescence intensity appeared after incubating with DHA@HPDA-Fe for 12 h.

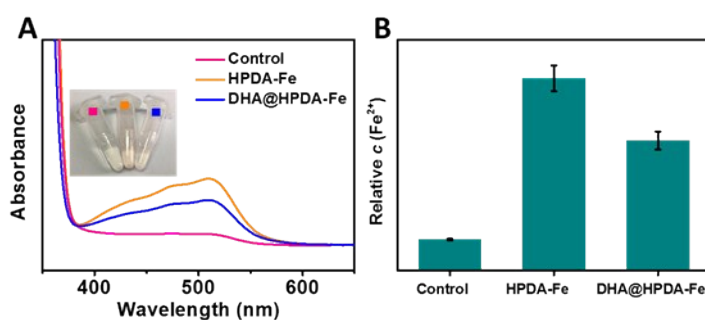


Figure S12. Detection the increasing concentration of ferrous ions in Hela cells. (A) The UV-vis absorbance spectrum of the cells supernatant of each group after treated with o-phenanthroline. Inset: a corresponding samples photograph of each group). (B) The relative concentrations of Fe²⁺ in the cells after they were treated with DMEM, HPDA-Fe and DHA@HPDA-Fe, respectively.

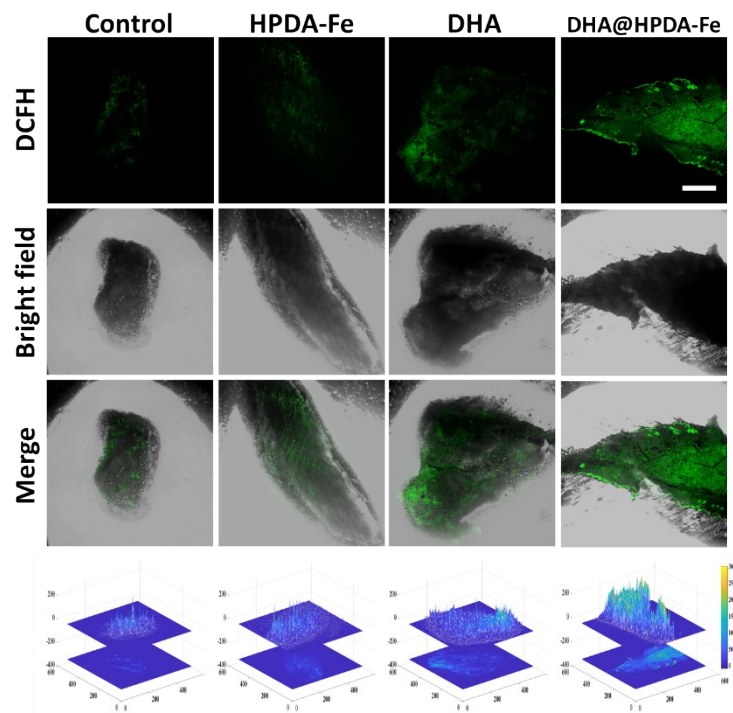


Figure S13. ROS stained tumor slices of the mice after the treatment of DMEM, HPDA-Fe, free DHA, and DHA@HPDA-Fe, respectively. Scale bar = 600 μ m.

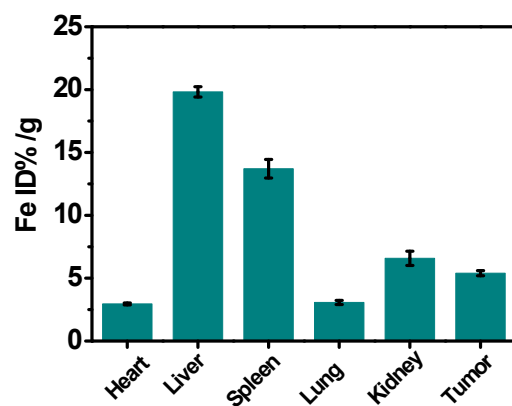


Figure S14. Biodistribution of DHA@HPDA-Fe nanospheres in major organs and tumor tissues at 24 h post intravenous injection evaluated by the content of Fe ions measuring with ICP.

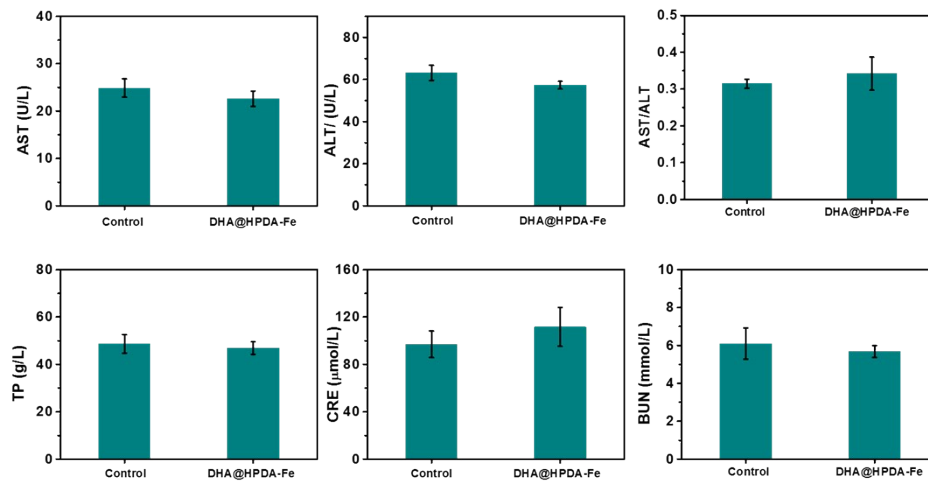


Figure S15. Blood biochemistry analysis of healthy mice (Control) or mice treated with DHA@HPDA-Fe nanospheres. The results showed the mean and standard deviations of aspartate aminotransferase (AST), alanine aminotransferase (ALT), AST/ALT ratio, total protein (TP), creatinine (CRE) and blood urea nitrogen (BUN).